



## Characterisation of fatty acyl reductases of sunflower (*Helianthus annuus* L.) seed

Cristina DeAndrés-Gil<sup>a</sup>, Antonio J. Moreno-Pérez<sup>a,b</sup>, Mónica Villoslada-Valbuena<sup>a</sup>, Kirstie Halsey<sup>c</sup>, Enrique Martínez-Force<sup>a</sup>, Rafael Garcés<sup>a</sup>, Smita Kurup<sup>c</sup>, Frédéric Beaudoin<sup>c</sup>, Joaquín J. Salas<sup>a</sup>, Mónica Venegas-Calero<sup>a,\*</sup>

<sup>a</sup> Instituto de la Grasa (CSIC), Ctra. Utrera Km 1, Building 46, 41013 Sevilla, Spain

<sup>b</sup> Departamento de Microbiología, Facultad de Biología, Universidad de Sevilla, 41012 Sevilla, Spain

<sup>c</sup> Plant Sciences Department, Rothamsted Research, Harpenden, United Kingdom

### ARTICLE INFO

#### Keywords:

Sunflower oil  
Wax ester  
Fatty acyl-CoA reductase  
FAR

### ABSTRACT

Long and very long chain fatty alcohols are produced from their corresponding acyl-CoAs through the activity of fatty acyl reductases (FARs). Fatty alcohols are important components of the cuticle that protects aerial plant organs, and they are metabolic intermediates in the synthesis of the wax esters in the hull of sunflower (*Helianthus annuus*) seeds. Genes encoding 4 different FARs (named *HaFAR2*, *HaFAR3*, *HaFAR4* and *HaFAR5*) were identified using BLAST, and studies showed that four of the genes were expressed in seed hulls. In this study, the structure and location of sunflower FAR proteins were determined. They were also expressed exogenously in *Saccharomyces cerevisiae* to evaluate their substrate specificity based on the fatty alcohols synthesized by the transformed yeasts. Three of the four enzymes tested showed activity in yeast. *HaFAR3* produced C18, C20 and C22 saturated alcohols, whereas *HaFAR4* and *HaFAR5* produced C24 and C26 saturated alcohols. The involvement of these genes in the synthesis of sunflower seed wax esters was addressed by considering the results obtained.

### 1. Introduction

Plant primary fatty alcohols are aliphatic compounds that are present either in their free form or as complex molecules, such as wax esters (WEs) or ether lipids (Dittrich-Domergue et al., 2014). In combination with other compounds, WEs and their derivatives form the lipid constituents of the cuticle barrier of plant organs. This barrier protects the plant from various biotic and abiotic stresses, such as UV light, drought or pathogen attack, and also limits non-stomatal water loss (Rowland and Domergue, 2012). Wax esters can also act as an energy storage reserves in some species, as seen in jojoba (*Simmondsia chinensis*) seed (Metz et al., 2000). Owing to the chemical and physical properties of WEs and fatty alcohols, they are used in a wide range of industrial products such as detergents, surfactants or lubricants (Domergue and Miklaszewska, 2022; Krishnan et al., 2020).

The primary very long chain alcohols, present in surface lipids, are synthesised via reduction of CoA esters of very long chain fatty acids (VLCFAs) by fatty acyl-CoA reductases (FARs) in NADPH-dependent

reactions. VLCFAs are formed by the fatty acyl-CoA elongase (FAE) system, through successive two carbon elongation cycles involving four enzymatic reactions (Fehling and Mukherjee, 1991). Therefore, the synthesised very long chain alcohols can be incorporated into the protective layer of aerial organs (Chibnall et al., 1934), particularly after esterification with activated fatty acids to produce WEs (Fig. S1; Lardizabal et al., 2000; Metz et al., 2000; Miklaszewska and Banaś, 2016). Fatty acyl-CoA reductases have been characterized in numerous plant species, such as jojoba (Metz et al., 2000; Miklaszewska and Banaś, 2016), *Arabidopsis thaliana* (Arabidopsis; Chacón et al., 2013; Domergue et al., 2010; Rowland et al., 2006), rice (*Oryza sativa*; Shi et al., 2011) and wheat (*Triticum aestivum*; Wang et al., 2015), as well as in mammals and microorganisms (Cheng and Russell, 2004; Willis et al., 2011). Fatty acyl-CoA reductase proteins have a Rossmann-fold domain at the N-terminus, which is involved in their binding to the NAD(P)H cofactor, and a specific fatty acyl-CoA reductase domain (FAR\_C) at the C-terminus that is yet to be attributed a clear role (Rowland and Domergue, 2012). The Rossmann-fold domain contains the conserved GXXGXX

\* Corresponding author.

E-mail address: [mvc@ig.csic.es](mailto:mvc@ig.csic.es) (M. Venegas-Calero).

<https://doi.org/10.1016/j.plantsci.2024.111992>

Received 28 July 2023; Received in revised form 2 January 2024; Accepted 14 January 2024

Available online 30 January 2024

0168-9452/© 2024 The Author(s). Published by Elsevier B.V. This is an open access article under the CC BY-NC-ND license (<http://creativecommons.org/licenses/by-nc-nd/4.0/>).

(G/A) motif (Wang et al., 2016) and the YXXXK active site motif, where tyrosine and lysine residues are predicted to play a direct role in catalysis as per the studies on other related reductases (Fujimoto et al., 2001).

In Arabidopsis, the FAR3/CER4 fatty acyl-CoA reductase generates significant amounts of primary alcohols that are associated with WEs production in the aerial organs (Rowland et al., 2006). The carbon chain lengths of the fatty alcohols range from C24:0-OH to C30:0-OH and the prevalent WEs have carbon chain lengths of C42–46. Heterologous expression of the FAR3/CER4 protein in yeast produces C24 and C26 primary alcohols. Moreover, *cer4* Arabidopsis mutants show considerably less C24 and C26 fatty alcohols and partially decreased C28 species, with a significant reduction in the predominant WEs in the stem cuticle. This result is consistent with the alcohols produced by yeast expressing CER4 and indicates that C24–C28 chain length alcohols are produced specifically by CER4 (Rowland et al., 2006; Rowland and Domergue, 2012).

In sunflower (*Helianthus annuus*), WEs are minor components of the economically relevant sunflower oils (Broughton et al., 2018). Sunflower oil is one of the most widely used seed oils (Salas, Bootello and Garcés, 2015) and its waxes are partially removed during oil refining as they tend to crystallize at room temperature and make the oil turbid (Chalapun et al., 2017). The main crude wax components obtained from refined sunflower seed oil are WEs with carbon chains between C38–C54, predominantly C42 (Garcés et al., 2023; Kanya et al., 2007; Kleiman et al., 1969). Comparable results were obtained with the WEs isolated from the seed hull and purified sunflower wax (Kanya et al., 2007; Kleiman et al., 1969; Rivarola et al., 1985). Indeed, the main alcohols in sunflower wax have chain lengths of C22, C24 and C26, whereas the main acids have chain lengths of C20 and C22 (Kanya et al., 2007).

In this study, we cloned and characterised the genes encoding four putative fatty acyl-CoA reductases from sunflower seeds that were named *HaFAR2*, *HaFAR3*, *HaFAR4* and *HaFAR5*. The activities of these enzymes were evaluated via heterologous expression in yeast and the subcellular distribution of the corresponding fluorescent labelled FAR proteins was investigated after transient-expression in tobacco leaves. The role of these genes in the biosynthesis of very long chain fatty alcohols, that are needed to produce WEs in sunflower seeds, was addressed.

## 2. Materials and methods

### 2.1. Biological material and growth conditions

CAS-6 sunflower line (Sunflower Collection of the Instituto de la Grasa, CSIC, Seville, Spain) and *Nicotiana benthamiana* Domin. plants were grown in chambers at 25 °C/15 °C and 22 °C/20 °C (day/night cycles), respectively, with a 16 h photoperiod and a photon flux density of 250  $\mu\text{mol m}^{-2}\text{s}^{-1}$ . The seeds from sunflower plants were harvested at different developmental stages (4, 7, 10, 12, 18, 25 days after anthesis (DAA)), and seeds from 4 to 10 DAA were used whole, whereas those from 12 to 25 DAA were separated into kernel and hull. Vegetative tissues used in expression studies (leaf, stem, roots and cotyledons) were collected 6 days after germination, and all tissues were frozen in liquid nitrogen and stored at -80 °C until RNA extraction.

*Escherichia coli* DH5 $\alpha$  strain was used as the host for gene cloning, whereas the *Agrobacterium tumefaciens* strain GV3101 was used for agroinfiltration and transient expression in tobacco leaves. *Saccharomyces cerevisiae* W303–1A strain (*MATa ade2–1 his3–11,15 leu2–3112 trp1–1 ura3–1*) and TDY7002 *elo3 $\Delta$  mutant strain (*MATa ura3–52 trp1  $\Delta$  leu2  $\Delta$  elo3::TRP1*) (Paul et al., 2006) were used as heterologous expression systems to assess specificity and function.*

### 2.2. mRNA isolation and cDNA synthesis

Approximately 0.4 g of sunflower seeds or vegetative tissues were ground in liquid nitrogen using a precooled sterile mortar and pestle. The Spectrum Plant Total RNA Kit (Sigma-Aldrich, Saint Louis, MO) was

used to isolate total RNA from all tissues except the seed hulls via the cetyltrimethylammonium bromide method (Chang et al., 1993) to extract total RNA from the hulls. The corresponding cDNAs were synthesised using the Ready-To-Go T-Primed First-Strand Kit (GE Healthcare, Chicago, IL).

### 2.3. Gene expression studies using RT-qPCR

The cDNA obtained from the different sunflower tissues were amplified by real-time quantitative PCR (RT-qPCR; see Moreno-Pérez et al., 2021) using specific primer pairs (Table S1; all primers were synthesized by Eurofins MWG Operon, Germany). The Livak method (Livak and Schmittgen, 2001) was used to calculate the relative expression of the genes in the samples and the sunflower *HaACT1* actin gene (GenBank Accession FJ487620) was used as a calibrator gene for normalization and amplified using specific *HaActin-F4* and *HaActin-R4* primers (Table S1). The efficiency and specificity of the primer pairs to amplify the *HaFAR1* (qPCR\_ *HaFAR1\_F*/qPCR\_ *HaFAR1\_R*) and *HaFAR6* (qPCR\_ *HaFAR6\_F*/qPCR\_ *HaFAR6\_R*) genes was below the threshold for inclusion in the study; thus, the expression level of these genes could not be analysed.

### 2.4. Gene cloning

Arabidopsis FAR3/CER4 protein sequence (At4g33790) was used to identify genes encoding sunflower FARs, by searching for sequence similarities in the Heliogene sunflower database (Sunflower genome portal, Heliogene - <https://www.heliogene.org>, Badouin et al., 2017) using the tblastn tool (Camacho et al., 2009). Four homologous sunflower FAR genes were selected (*HaFAR2*, *HaFAR3*, *HaFAR4* and *HaFAR5*) and their coding regions were amplified using PCR from the developing sunflower seed cDNA using specific primers for each vector (Table S1). The nucleotide sequences were confirmed using sequencing (Eurofins MWG Operon, Germany).

### 2.5. Sequence analysis and phylogenetic tree construction

The deduced amino acid sequences of the *HaFAR* proteins were aligned with homologous proteins from other plant species and retrieved from the NCBI database using the BLASTP program (<http://www.ncbi.nlm.nih.gov/>). The amino acid sequences were aligned using the Clustal Omega tool service from EMBL-EBI (Madeira et al., 2022) under the default settings. Further modifications of the alignments were carried out using the Bioedit Sequence Alignment Editor software (Hall, 1999). These alignments were used to generate a phylogenetic tree based on the neighbour-joining algorithm (Saitou and Nei, 1987) using the MEGA X software (Kumar et al., 2018), implementing a bootstrap test with 10,000 replicates. The InterPro (Paysan-Lafosse et al., 2023) and PROSITE (Cuče et al., 2013) protein databases were used to obtain information on the conserved domains and functional sites in the *HaFARs* and to identify them as members of a known superfamily. The transmembrane domains were predicted using the DeepTMHMM (Hallgren et al., 2022) and HMMTOP 2.0 (Tusnády and Simon, 2001) prediction software, and the subcellular localisation was predicted via MultiLoc2 (Blum et al., 2009) and DeepLoc 2.0 (Thumuluri et al., 2022).

### 2.6. Modelling of the HaFAR three-dimensional structures

The putative *HaFAR2*, *HaFAR3*, *HaFAR4* and *HaFAR5* protein structures were homology-modelled using the AlphaFold server (Jumper et al., 2021; <https://alphafold.ebi.ac.uk/>). Molecular docking was performed with SwissDock (Grosdidier et al., 2011a, 2011b; <http://www.swissdock.ch/>) using docosanoyl-CoA (C22:0-CoA) as the substrate and employing the default parameters. Structures were visualised and residues were mapped using the UCSF Chimera package (Pettersen et al., 2004).

## 2.7. Construction of yeast expression plasmids and expression in yeast

The coding regions of the selected *HaFAR* genes were expressed heterologously in yeast using the pYES2 expression vector under the control of a GAL1 promoter (Thermo Fisher Scientific, USA). The *HaFAR* genes were amplified using primers including restriction sites for *Bam*HI and *Xho*I (Table S1), and the amplified products were digested and ligated into the corresponding restriction sites in pYES2. The recombinant plasmids were sequenced and transformed into the *S. cerevisiae* W303–1A yeast strain or the *elo3Δ* mutant strain using the PLATE method (Becker and Lundblad, 1994).

W303–1A yeast transformants were screened using synthetic complete (SC) media plates lacking uracil (SC-Ura), whereas *elo3Δ* transformants were screened using SC media lacking uracil and tryptophan (SC-Ura-Trp). Colonies containing the different constructs, or the empty vector alone as a control, were inoculated separately into SC-Ura or SC-Ura-Trp liquid medium containing 2% (w/v) raffinose and grown overnight at 30 °C. The cultures were then diluted (OD<sub>600</sub> = 0.2) in 100 mL of medium supplemented with 1% (w/v) raffinose and 2% (w/v) galactose to induce expression, and incubated for 2 days prior to lipid extraction.

## 2.8. Analysis of fatty alcohol synthesis in transgenic yeast

The yeast cells were harvested by centrifugation at 1500 × g at 4 °C for 5 min, washed with distilled water and the cell pellet was dried under a gentle stream of nitrogen. Heneicosanoic alcohol (C21:0-OH, 20 μg) was added as an internal standard and the total lipids from the cells were extracted (Bligh and Dyer, 1959) and evaporated under nitrogen. Fatty acid methyl esters (FAMES) were obtained by transmethylation with methanol/toluene/sulfuric acid (88/10/2, v/v/v) at 85 °C for 1 h. After cooling, 3 mL of hexane was added and the fatty acyl chains were extracted, by drying the extracts under nitrogen and then dissolving them in hexane: diethylether (95:5, v/v). Fatty alcohols were separated from the FAMES via solid phase extraction on a Lichrolut 0.5 g silica gel cartridge (Merck) using a vacuum manifold. FAMES were eluted by adding 8 mL of hexane: diethylether (95:5, v/v), and the fatty alcohols were eluted with 8 mL of hexane: ethyl acetate (6:1, v/v). Fatty alcohol extracts were dried and dissolved in 100 μL of N,O-bis(trimethylsilyl)-trifluoroacetamide (BSTFA)/trimethylchlorosilane (TMCS, 98:2) and incubated at 85 °C for 1 h to facilitate silylation of any free hydroxyl groups. The samples were evaporated under nitrogen and resuspended in 200 μL of heptane before GC/MS analysis.

## 2.9. GC/MS analysis

The silylated fatty alcohols were separated and analysed using an Agilent 8890 GC/MS system in split mode, endowed with a Quadrex 007–65HT mid-polar capillary column (30 m × 0.25 mm and a 0.10 μm phase), with the injector set at 340 °C, and using H<sub>2</sub> as the carrier gas at a flow rate of 1.6 mL/min. Injection was performed using a split ratio of 1:20. The oven was programmed at an initial temperature of 230 °C, which was maintained for 5 min, and then increased to 330 °C at a rate of 2 °C/min. The MS Agilent 5977B detector was initially set in scan mode in a m/w range of 145–905 and with no integration of peaks smaller than 0.2%. For the selected ion monitoring (SIM) mode, the detector was set to the specific molecular ion using the precise window for each silylated alcohol species (± 0.5 Da) and considering their retention times. Quantification was carried out based on the area of the peaks in relation to the area of the 21:0-TMS internal standard.

## 2.10. Transient expression in *Nicotiana benthamiana*

For transient expression in tobacco leaves, the *HaFAR* coding regions without a stop codon were amplified from sunflower seed cDNA via PCR using the primers listed in Table S1. The amplified fragments were cloned

into the pENTR/D-TOPO vector using the pENTR Directional TOPO Cloning Kit (Invitrogen). The products were then transferred to the pK7FWG2 vector (Karimi et al., 2002, 2007) using the GATEWAY recombination cloning system (ThermoFisher Scientific, USA) at the attL x attR (LR) recombination sites. This vector allows C-terminal fusion of the protein of interest with green fluorescent protein (GFP) at the C-terminal end, generating GFP/*FAR* fusion constructs (Fig. S2). The RanBP1 protein from *Nicotiana benthamiana* fused to the red fluorescent protein (RFP) using the pK7RWG2 vector acted as the cytosolic marker (Cho et al., 2008), and the endoplasmic reticulum (ER) membrane marker CD3–959-mCherry was used as the ER marker (Nelson et al., 2007). The constructs were cloned in *E. coli* and then transferred to the *Agrobacterium tumefaciens* GV3101 strain using the freeze-thaw method. Tobacco leaves were transformed via agroinfiltration using the 35 S:p19 viral suppressor construct (Moreno-Perez et al., 2014), and the transformed plants were incubated under normal growth conditions for 4 days and analysed using a Leica Stellaris FALCON confocal laser-scanning microscope (Leica Microsystems, Germany) using a x40 water immersion objective. To image the fluorescently tagged proteins, cells were excited with an argon laser at 488 nm (GFP) and 587 nm (RFP and mCherry), and fluorescence emission was detected between 490–540 nm for GFP, and 590–640 nm for RFP and mCherry. Image processing was carried out using the Leica LAS X software (Leica Microsystems, Germany).

## 3. Results

### 3.1. Grouping of eight sunflower *FAR* genes into three families

The sunflower genome was examined to assess for the presence of genes likely to encode fatty acyl-CoA reductases. The coding sequences were searched using BLAST and other resources available at the sunflower ‘Heliagene’ genome portal using the Arabidopsis *FAR3/CER4* protein sequence (At4g33790) as the template. This search identified 8 full-length genes encoding sequences that had significant similarity to *FAR3/CER4*, with 40–58% amino acid sequence identity. These *HaFAR* genes were designated *HaFAR1* to *HaFAR8* and their nucleotide sequences were aligned (see Table 1 for their GenBank accession numbers and Fig. S3).

The deduced protein sequences of the 8 putative fatty acyl-CoA reductases were situated in a phylogenetic tree together with other known *FAR* proteins (Fig. 1). A neighbour-joining (NJ) method with bootstrap analysis was implemented using the MEGA X software (Kumar et al., 2018), a bootstrap test with 10,000 replicates. Two *FARs* from *Monoraphidium neglectum* (green algae) were used to root the tree. This analysis showed that the 8 sunflower *FARs* clustered into two groups. The sunflower proteins *HaFAR1* to *HaFAR5* belonged to the first clade, close to the *AtFAR3/CER4* proteins from Arabidopsis, *CsFAR3* from *Camelina sativa*, *ScFAR* from jojoba, *VvFAR3* from *Vitis vinifera* and *RcFAR3* from *Ricinus communis*. The *HaFAR6* protein was also included in this clade related to *AtFAR3/CER4*, but grouped in a different branch. Another clade included *HaFAR7* and *HaFAR8* along with *AtFAR2* and

**Table 1**  
GenBank accession numbers and protein information of the sunflower *FARs*.

Gene name	GenBank Accession No.	CDS length (bp)	Protein information		
			No. Aas	MW (kDa)	PI
<i>HaFAR1</i>	XM_022150025	1473	490	55.01	8.53
<i>HaFAR2</i>	XM_022149996	1479	492	54.91	8.35
<i>HaFAR3</i>	XM_022117753	1476	491	55	8.50
<i>HaFAR4</i>	XM_022141724	1479	492	56.03	8.87
<i>HaFAR5</i>	XM_022144823	1479	492	55.55	8.07
<i>HaFAR6</i>	XM_022132495	1476	491	55.89	8.83
<i>HaFAR7</i>	XM_022127761	1821	606	67.45	8.81
<i>HaFAR8</i>	XM_022143739	1806	601	67.03	9.02

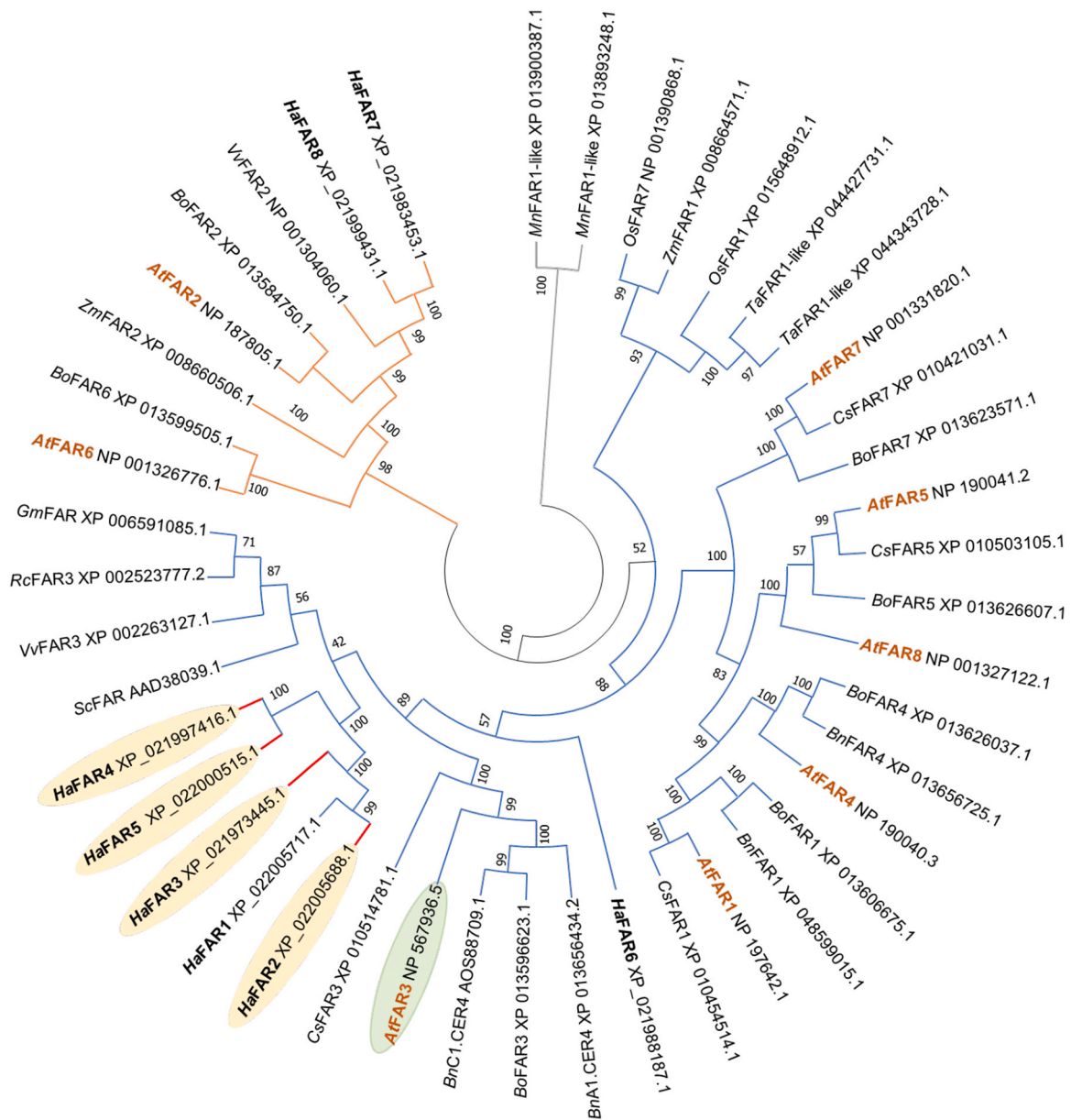


**Fig. 1.** Phylogenetic tree of plant FAR enzymes. The plant species included in the phylogenetic tree are from: *At*, *Arabidopsis thaliana*; *Bn*, *Brassica napus*; *Bo*, *Brassica oleracea*; *Br*, *Brassica rapa*; *Cs*, *Camelina sativa*; *Gm*, *Glycine max*; *Ha*, *Helianthus annuus*; *Os*, *Oryza sativa*; *Rc*, *Ricinus communis*; *Sc*, *S. chinensis*; *Vv*, *Vitis vinifera*; *Zm*, *Zea mays*. The green algae *M. neglectum* was used as an outlying group to root the tree (light grey). The sunflower FARs are marked in bold, and *HaFAR2*, *HaFAR3*, *HaFAR4* and *HaFAR5* are indicated with a red line. Arabidopsis forms were marked in orange colour.

*AtFAR6*, and other related FARs from *Zea mays*, *Vitis vinifera* or *Brassica oleracea*.

The amino acid sequences of *HaFAR2*, *HaFAR3*, *HaFAR4* and *HaFAR5* were aligned to reference proteins from different species: *AtFAR3*/CER4 from *Arabidopsis*, *RcFAR3* from *Ricinus communis* and *ScFAR* from *jojoba* (Fig. S4). The four sunflower proteins were very similar, with identities ranging from 70 to 85% in their amino acid sequences, and a 58% identity with FAR3/CER4 from *Arabidopsis*. All FAR proteins had a highly conserved GXXGXX(G/A) motif in a NAD(P)H-binding Rossmann-fold domain and a conserved YXXXK motif at the active site (Fig. S4).

### 3.2. *HaFAR2* was the most expressed FAR gene in sunflower seeds

The data gathered from a publicly available sunflower transcriptomic database (Badouin et al., 2017) confirmed the expression of

*HaFAR* genes from the first clade in different organs. To confirm and amplify these data, the expression of the sunflower FAR genes in different sunflower tissues, including stems, leaves, cotyledons, roots and seeds at different developmental stages, was analysed using RT-qPCR. This first clade included the FARs related to the *Arabidopsis* FAR3/CER4 gene, *HaFAR1*, *HaFAR2*, *HaFAR3*, *HaFAR4* and *HaFAR5*. *HaFAR1* and *HaFAR6* were not included in the study because we could not obtain specific oligomeric primers with the required amplification efficiency. A similar pattern of expression was evident for all other genes, with stronger expression in the hulls than in the seed kernels (Fig. 2). *HaFAR2* was the most strongly expressed sunflower FAR gene in seeds, reaching a peak at 10 DAA and decreasing in hulls in later stages, but with no significant expression in the seed kernels. The expression of *HaFAR3* followed a distinct pattern, with weak expression in early stages, from 4 to 10 DAA, and stronger expression as the seeds developed. In this case, the expression in the kernel was detectable at 18 DAA

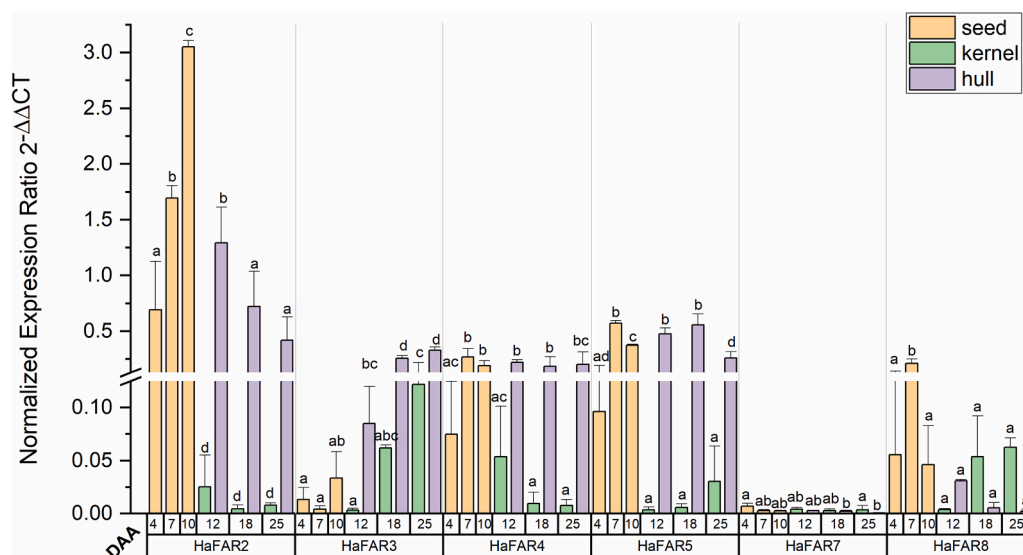


**Fig. 2.** Normalised expression ratio of sunflower FAR genes in the sunflower line CAS-6 at different stages of seed development. Expression was measured by RT-qPCR using the *Helianthus annuus* *HaACT1* actin gene (GenBank Accession FJ487620) as a reference gene. The data correspond to the mean  $\pm$  SD of three independent measurements. (a, b, c, d). Statistical significance according to one-way analysis of variance (ANOVA) with a Tukey's post hoc analysis at a significance level of 0.05.

or later. *HaFAR4* and *HaFAR5* were initially expressed in a similar pattern, with high levels of expression in the early stages of development when the whole seed was analysed. When the kernel and hull were studied separately, the expression of both genes was much stronger in the hulls than in the seed kernels, and they were stably expressed during seed development. Regarding *HaFAR7* and *HaFAR8*, the expression of *HaFAR7* was very weak in seeds at all stages of development, whereas *HaFAR8* was expressed at high levels in immature seeds (4 to 10 DAA); considering the data in Fig. 2, the expression appeared to decrease in the hull and increase in the kernel during seed development.

### 3.3. Heterologous expression of *HaFAR3*, *HaFAR4* or *HaFAR5* produced fatty alcohols in yeast

To learn more about the biochemical properties and role of sunflower seed FARs in WE synthesis, four genes were selected as candidates believed to be involved in WE synthesis, *HaFAR2*, *HaFAR3*, *HaFAR4* and *HaFAR5*, based on their homology to the Arabidopsis FAR3/CER4 gene and their expression in the seed. To express these genes in yeast, their open reading frames (ORFs) of 1479 bp (*HaFAR2*), 1476 bp (*HaFAR3*), 1479 bp (*HaFAR4*) and 1479 bp (*HaFAR5*) were amplified from 10 DAA developing sunflower seed cDNAs using specific primers, cloning these ORFs into the pYES2 vector. These sequences correspond to the reference sequences HanXRQr2Chr14g0655621 (*HaFAR2*), HanXRQr2Chr07g0306271 (*HaFAR3*), HanXRQr2.Chr02g0080711 (*HaFAR4*) and HanXRQr2Chr13g0581011 (*HaFAR5*) from the sunflower genome (Badouin et al., 2017), and they encode proteins of 492, 491, 492 and 492 amino acids, with predicted molecular weights of 54.91, 55, 56.03 and 55.55 kDa, and with pI values of 8.35, 8.5, 8.88 and 8.07, respectively.

The resulting constructs were introduced into the wild-type (WT) W303-1A *S. cerevisiae* and *elo3Δ* mutant strain (Paul et al., 2006), using the empty vector as a negative control in each case. Following induction, transgenic WT yeast expressing *HaFAR3*, *HaFAR4* or *HaFAR5* produced fatty alcohols up to C26:0-OH, at approximately 65, 260 and 320  $\mu$ g/g dry weight, respectively, whereas yeast expressing *HaFAR2* produced no significant increments of fatty alcohols (Fig. 3A). In terms of the composition of the fatty alcohols produced by W303-1A yeast, there was no change in the fatty alcohol composition of the strain expressing

*HaFAR2* (Fig. 3B). Contrastingly, heterologous expression of *HaFAR3* resulted in significant production of C18:0-OH and 20:0-OH relative to the yeast expressing the empty vector, whereas *HaFAR4* and *HaFAR5* expression led to significant C24:0-OH and C26:0-OH production compared to the controls. The expression of these constructs in the yeast *elo3Δ* mutant was also analysed to assess their influence on long and very long chain fatty alcohol production, as the fatty acid elongation system in this mutant is altered leading to the accumulation of C22:0 FA and a small amount of C24:0 FA (Tables S2 and S3). When expressed in this mutant yeast strain, *HaFAR3* led to the accumulation of approximately 90  $\mu$ g/g dry weight of fatty alcohols (Fig. 4A), mainly comprising C22:0-OH with a small amount of C20:0-OH, differing significantly from the control. The *HaFAR4* construct also produced significantly more C22:0-OH and C24:0-OH fatty alcohols in the *elo3Δ* mutant than that in the control (Fig. 4B), in contrast to the mutant lines expressing *HaFAR2* and *HaFAR5* in which fatty alcohol production did not differ significantly from that of the control. The case of *HaFAR5* is especially interesting, because this result indicates that it displays very low activity towards acyl-CoAs of C22 or shorter.

### 3.4. Modelled sunflower FAR proteins highlighted the hydrophobic pocket required for protein activity

To explain the lack of activity in yeast, the 3D structure and functional domains of these proteins were studied. Three-dimensional structural representations of *HaFAR2*, *HaFAR3*, *HaFAR4* and *HaFAR5* were obtained via homology-modelling using AlphaFold and their amino acid sequences as a template. Molecular docking was performed using SwissDock software, using docosanoyl-CoA (C22:0-CoA) as a substrate and NADPH as a cofactor. As indicated, the *HaFAR* secondary structure consisted of two domains: a N-terminal domain/Rossmann-fold domain from residue 17 to 319; and the C-terminal domain comprising approximately 394 to 492 amino acids (Fig. 5). The NAD(P)H-binding site in the N-terminal domain is highly conserved in all four *HaFARs*, and residues G19-A25 in *HaFAR2*, *HaFAR3* and *HaFAR4*, or G20-A26 in *HaFAR5* constitute the GXXGXX(G/A) Rossmann-fold motif. In the N-terminal domain the conserved active site motif can be found, corresponding to residues Y238 and K242 of *HaFAR2*, *HaFAR3* and *HaFAR4*, and Y239 and K243 of *HaFAR5* (Fig. 6 A-D). Docking analysis of the four

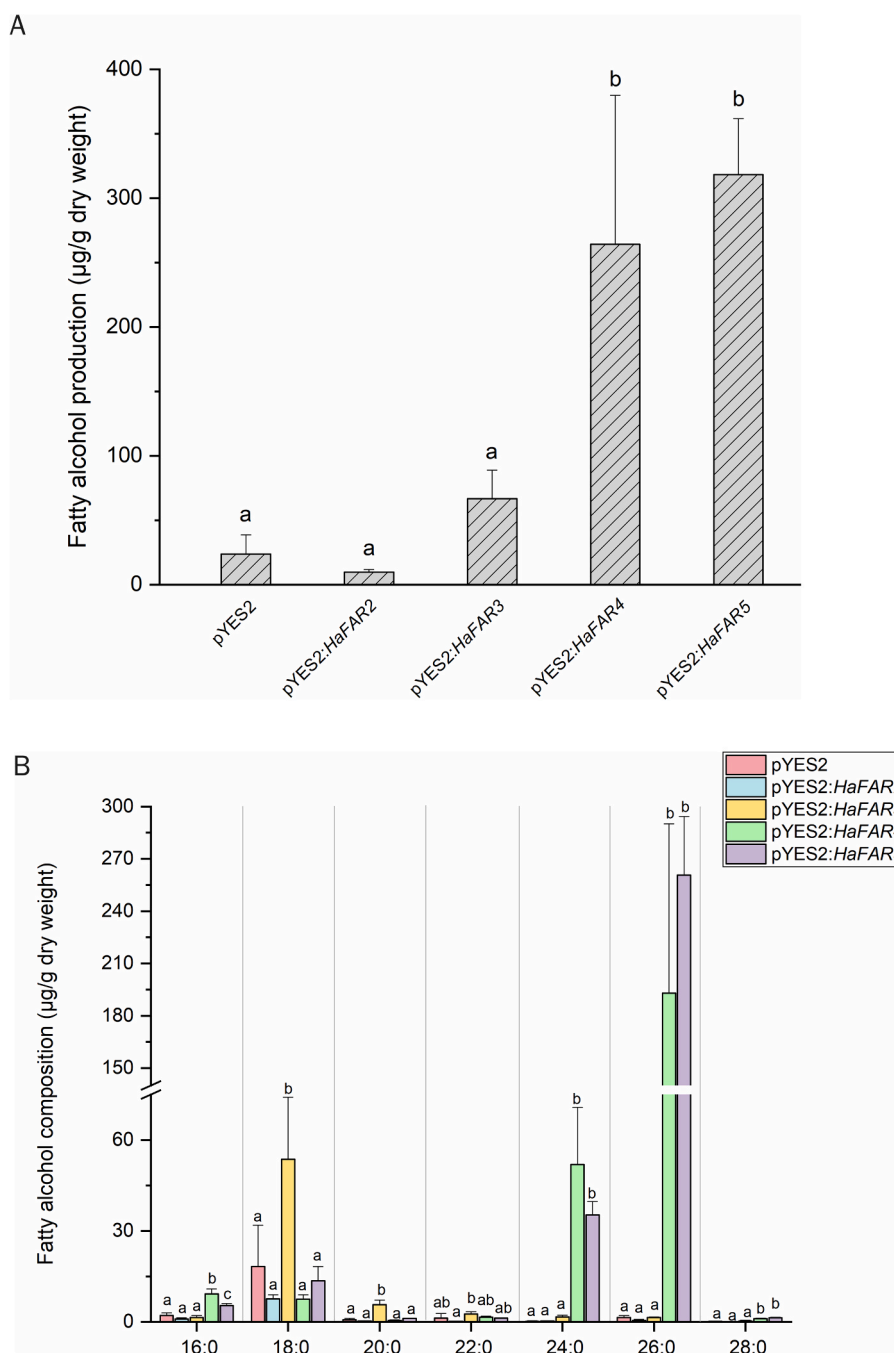


**Fig. 3.** Analysis of the fatty alcohols produced in the WT W303–1A yeast strain expressing *HaFAR2*, *HaFAR3*, *HaFAR4* and *HaFAR5* under the control of a *GAL1* promoter. The empty vector pYES2 was used as a negative control. **(A)** Quantification of the amount of primary fatty alcohols produced by FAR in µg/g dry weight. **(B)** Changes in the composition of fatty alcohols (standardised data in µg/g dry weight). The data correspond to the mean ± standard deviation of 3–4 independent replicates. (a, b, c, d) Statistical significance according to one-way analysis of variance (ANOVA) with Tukey's post hoc analysis at a significance level of 0.05.

modelled proteins highlighted a hydrophobic pocket that could simultaneously hold the acyl-CoA substrate and NADPH cofactor required for protein activity (Fig. 6 E–H, Fig. 7, Fig. S5).

### 3.5. *HaFARs* localisation studies

To study the subcellular localisation of *HaFAR*, the cytosolic marker *NbRanBP1* and ORFs lacking a STOP codon were transferred to Gateway compatible binary vectors to generate *HaFAR*-GFP and *NbRanBP1*-RFP constructs. Transient expression of these constructs in tobacco plants was monitored using confocal microscopy, and the fluorescence analysis of *HaFARs* showed partial co-localisation with the signal obtained from

*RanBP1*-RFP (cytosolic marker) and CD3–959-mCherry (ER marker). All three FAR-GFP constructs were localised in parts of the ER (Fig. 8B), although there was stronger colocalization with the cytosolic marker (Figs. 8A and S6).

## 4. Discussion

Fatty alcohols are important intermediates and components of the protective layer that plants use to avoid moisture loss from aerial organs and pest attack. In sunflower, the seed hulls are rich in saturated high melting point WEs (C40 to C60) that protect the embryo (Garcés et al., 2023), but the WEs interfere with the extraction and refining of

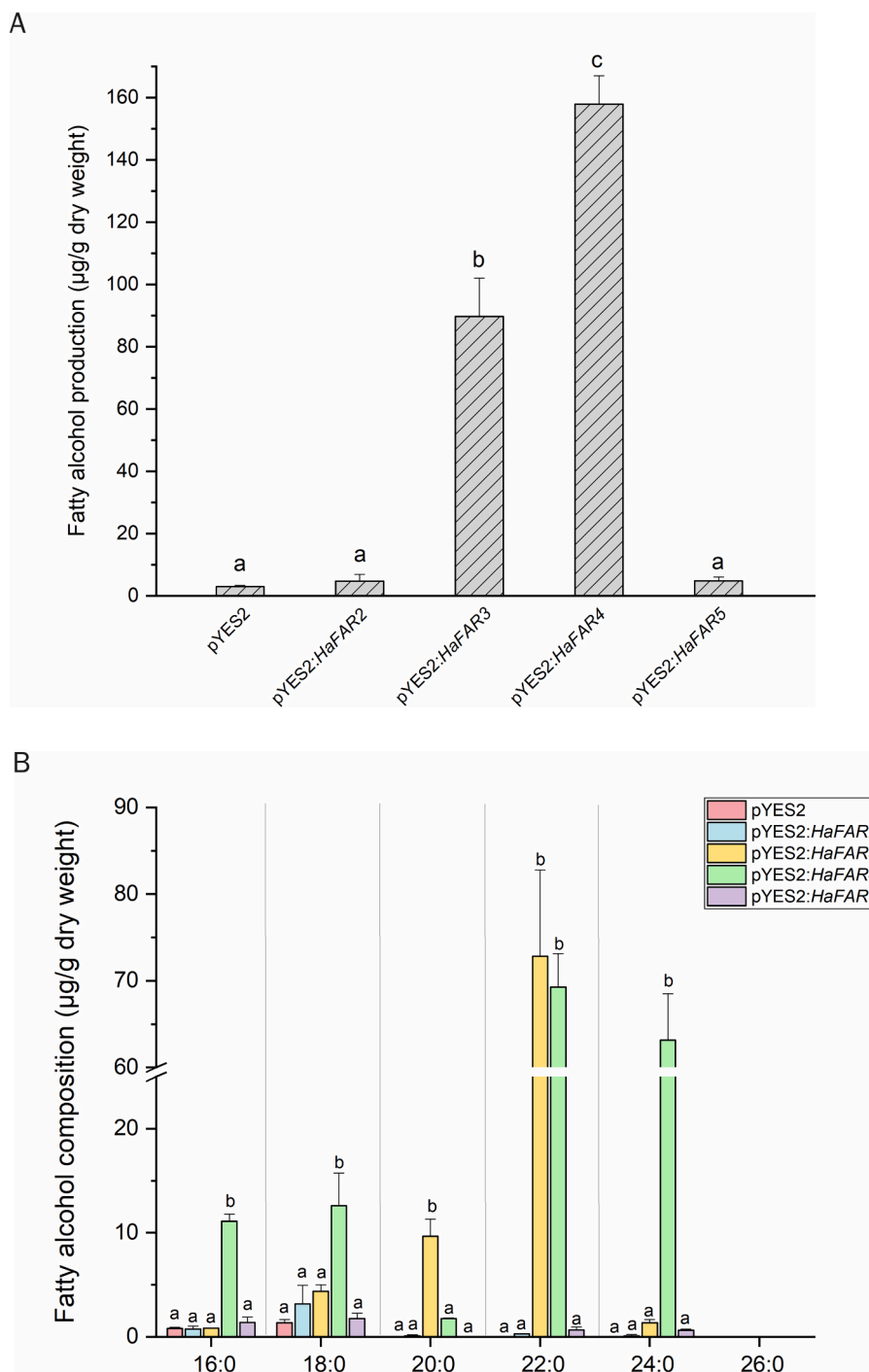


**Fig. 4.** Analysis of the fatty alcohols produced by the *elo3*Δ mutants expressing *HaFAR2*, *HaFAR3*, *HaFAR4* or *HaFAR5* under the control of a *GAL1* promoter. The empty vector pYES2 was used as a negative control. **(A)** Quantification of the primary fatty alcohols produced by FARs in µg/g dry weight. **(B)** Changes in the composition of fatty alcohols (standardised data in µg/g dry weight) in the *elo3*Δ mutant strain. (a, b, c) Statistical significance according to one-way ANOVA with Tukey's post hoc analysis at a significance level of 0.05.

sunflower oil. The fatty alcohols present in these WEs are even-chained saturated species, predominantly comprising C22 to C28. We aimed to characterize different FAR proteins present in sunflower and assess their contribution to WEs synthesis in sunflower seeds and oil.

Initially, the public sunflower gene database Heliagene was screened for sunflower genes homologous to the Arabidopsis gene *AtFAR3/CER4*, which encodes a fatty acyl-CoA reductase involved in WEs synthesis (Rowland et al., 2006). This gene was shown to synthesise saturated alcohols with C-chains in the range of C24 to C26. The fatty alcohols in the WEs of sunflower seeds ranged from C20 to C26 (Garcés et al., 2023).

Therefore, a certain degree of similarity between the genes in both species was expected. This search yielded 8 sunflower genes similar to *AtFAR3*, which were selected as candidates that were probably involved in sunflower fatty alcohol synthesis.

The phylogenetic study using representative FARs from several plant species separated the sunflower FARs into 2 clusters. The first included the forms, *HaFAR1* to *HaFAR5*, that were the closest or most similar to *AtFAR3*. These peptides were also the most similar to the FARs from jojoba (*S. chinensis*), *Vitis vinifera* and *Ricinus communis*. *HaFAR6* was also included in this cluster, although it branches out separately,

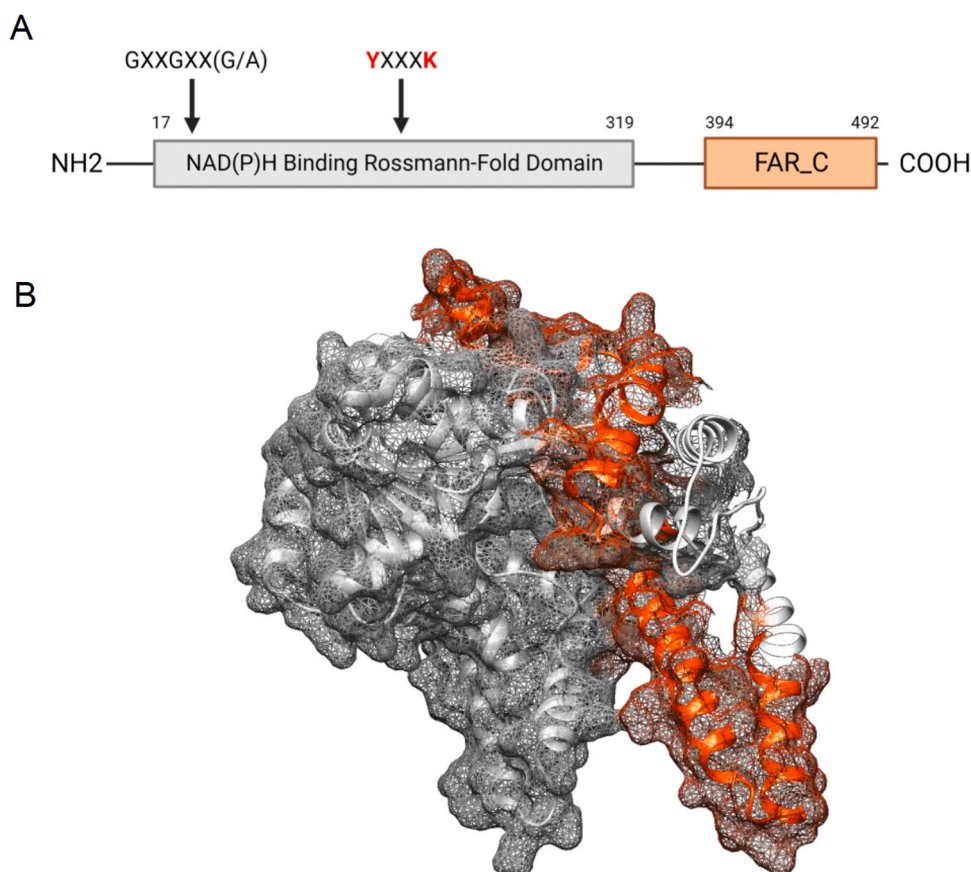


**Fig. 5.** Predicted *HaFAR* functional domains. **(A)** Overview of the structural domains of the FAR proteins, including a Rossmann-fold domain at the N terminus and fatty acyl-CoA reductase (FAR\_C) domain at the C terminus. Additionally, the Rossmann-fold domain contains two conserved motifs, an NAD(P)H binding site motif (GXXGXX(G/A)) and a YXXXK active site motif. The two catalytic residues of the active site motif TYR/LYS are indicated in red. **(B)** The tertiary structure of *HaFAR*2 showing the N terminal (grey) and C terminal domain (orange).

indicating a greater phylogenetic distance compared to the other members. Finally, the *HaFAR7* and *HaFAR8* isoforms clustered in another group close to the *AtFAR2* and *AtFAR6* Arabidopsis enzymes, which are located in plastids (Chen et al., 2011; Doan et al., 2012) and encode fatty acyl-acyl carrier protein (ACP) reductases required for the sporopollenin biosynthesis necessary for pollen wall differentiation (Aarts et al., 1997). This distribution was analogous to other species and is an example of the specialisation of enzymes with a common origin.

The pattern of the sunflower FAR gene expression was predicted using the information from the sunflower transcriptome database and to confirm these data, the expression of genes involved in WE synthesis was studied using RT-PCR in seed tissues at different stages of development. The transcription of *HaFAR2* to *HaFAR5* genes was determined and compared with those of *HaFAR7* and *HaFAR8* forms, which were not related to WE synthesis. This study was carried out on whole seeds from 4 to 10 DAA, and on the kernel and hull once these tissues differentiated, the seed formed and most of the surface lipids were synthesised (from 12 until 25 DAA). Among the 5 FAR analogues of *AtFAR3*, *HaFAR1* could not be studied as it was not possible to design specific oligonucleotides with the necessary efficiency. The pattern of expression differed greatly between the two gene families, with weak expression of the plastidial forms in the seed tissues. The FARs in the first clade were expressed more strongly in seeds. *HaFAR2* was expressed strongly in the initial stages of seed development, peaking at 10 DAA, after which it was expressed predominantly in the hull with only weak expression in the kernel. *HaFAR3* was expressed at later stages in the kernel and hull, whereas *HaFAR4* and *HaFAR5* were present at similar levels during seed formation, preferably expressed in the hull. These patterns of expression were coherent with the involvement of these genes in the synthesis of alcohols

present in sunflower seed WEs. Indeed, the saturated high molecular point waxes that were deposited in sunflower seeds accumulate in the hull (Garcés et al., 2023) and the 4 FARs were expressed in the seed hull at all stages, with only the *HaFAR3* gene expressed at similar levels in the seed kernel. The expression of *HaFAR3* in kernel could be due to fatty alcohol production for the synthesis of short esters other than those present in the hull and have been detected in sunflower seeds (Broughton et al., 2018) or of compounds other than WE. Previous studies on Arabidopsis showed stronger expression of *AtFAR3* in roots and open flowers (Rowland et al., 2006). Although the gene was expressed in siliques, no specific expression in different seed tissues was reported.

Among the FARs identified *HaFAR2*, *HaFAR3*, *HaFAR4* and *HaFAR5* were most similar to their Arabidopsis orthologue, encoding proteins of a similar size (491–492 aa; 54.91 to 56.03 kDa), with 58% identity and strongly expressed during sunflower seed development. To further characterize these genes, *HaFAR2*, *HaFAR3*, *HaFAR4* and *HaFAR5* were expressed heterologously in *S. cerevisiae* to examine their substrate specificity in terms of the fatty alcohols that they produce in the host. Different yeast preparations were tested, although no *in vitro* enzyme activity was detected when it was assayed (data not shown). The assay involved extraction of the total yeast lipids, followed by methylation and fatty alcohols separation in a silica gel cartridge. The fatty alcohols were then silanized and analysed using GC/MS in SIM mode for selective and accurate quantification. In the WT W303–1A yeast strain, only *HaFAR3*, *HaFAR4* and *HaFAR5* enhanced the total amount of fatty alcohol produced by the yeast, the latter exhibiting the highest increase of 300 µg/g dry weight. Control yeast lines showed traces of fatty alcohols that could have originated in the yeast host or from any kind of artefact or contamination. However, these did not alter the results obtained in this



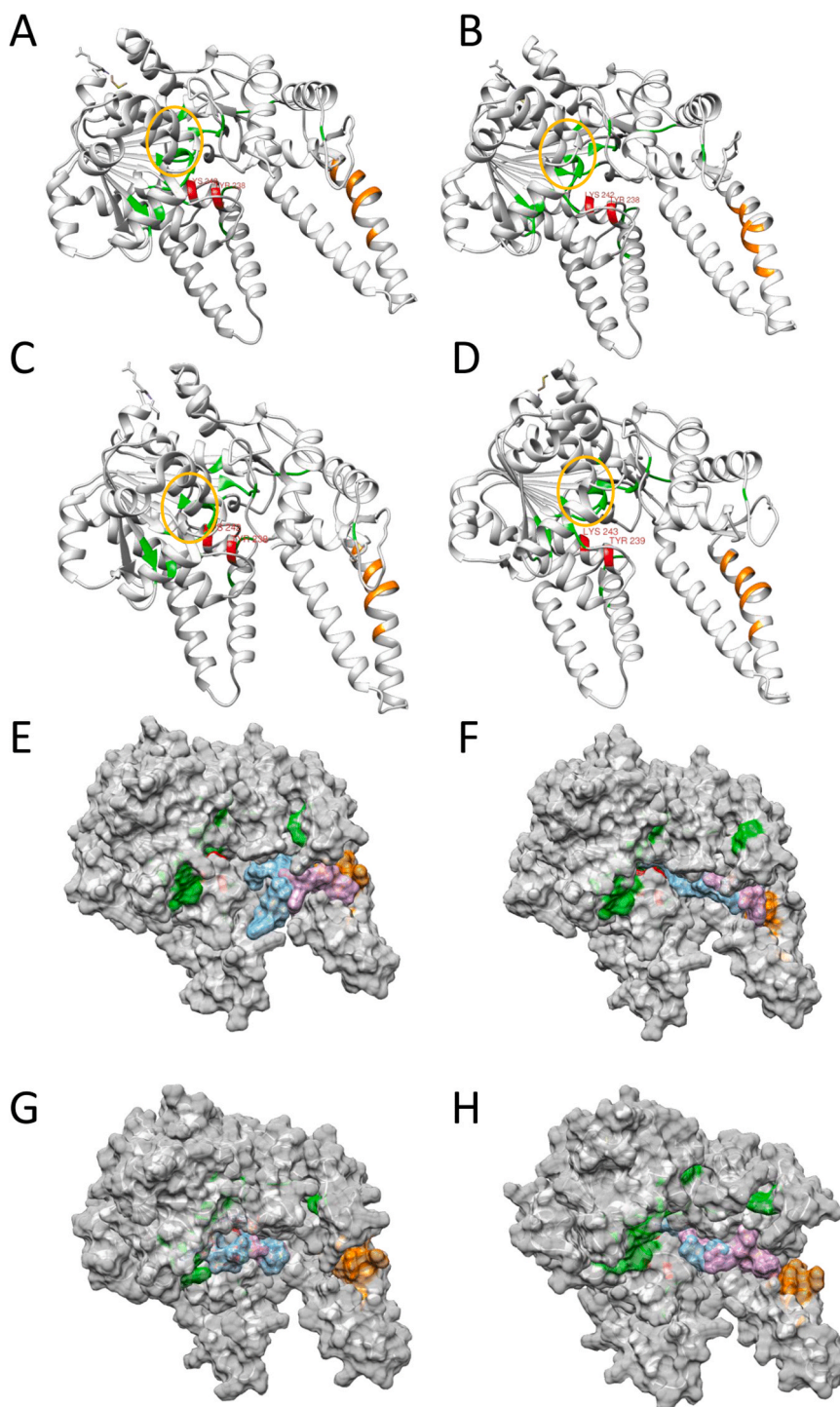


**Fig. 6.** Proposed structural models for *HaFAR2* (A, E), *HaFAR3* (B, F), *HaFAR4* (C, G) and *HaFAR5* (D, H). Ribbon diagrams (A, B, C, D). The hypothetical residues involved in substrate and cofactor binding are in green, and those involved in the catalytic activity of the enzymes are in red (FAR2 Y238, K242; FAR3 Y238, K242; FAR4 Y238, K242 and FAR5 Y239, K243). The residues marked in orange could form a hydrophobic surface that may interact with the substrate. The conserved GXXGXX(G/A) Rossmann-fold motif is circled in orange. (E, F, G, H) Surface computing of *HaFARs*. Molecular docking of the docosanoyl-CoA (C22:0-CoA) substrate (light blue) and NADPH cofactor (pink) in the *HaFAR* binding pockets.

series of experiments. The alcohols produced by this *HaFAR* were predominantly 24:0 and 26:0, whereas *HaFAR3* produced fewer alcohols, mainly 18:0 with smaller amounts of 20:0 fatty alcohols. Like *HaFAR5*, *HaFAR4* mainly led to the production of 24:0 and 26:0 fatty alcohols. Thus, the major FARs producing the saturated very long chain alcohols present in sunflower surface WEs appeared to be *HaFAR4* and *HaFAR5*, with a weaker contribution from *HaFAR3*.

*HaFAR2* was the gene expressed most strongly in the hull of sunflower seed but it displayed no activity in yeast. This could be because it was not functional or active in the *S. cerevisiae* expression system, which should be confirmed in a plant system or by complementation of plant mutants. Moreover, one of the most abundant fatty alcohols in the sunflower seed hull is 22:0, and none of the active *HaFARs* studied here produced this alcohol in large proportions in the WT W303-1A yeast

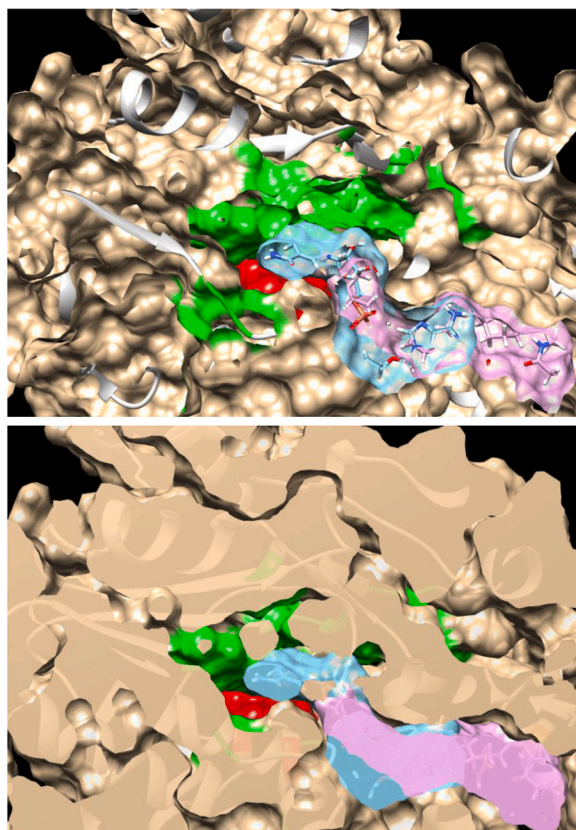


**Fig. 7.** Slab views of the substrate binding pocket proposed for *HaFAR5*. Molecular docking with docosanoyl-CoA substrate (light blue) and NADPH cofactor (pink) is shown. The residues involved in the substrate and cofactor interaction are shown in green, and those involved in catalysis are in red.

strain. This could reflect the substrate specificity of the enzymes assayed and/or the composition of the acyl-CoA pool in the yeast host. Yeast has previously been reported to possess elongases that act on 22:0-CoA, and that deploy the 22:0-CoA acyl-CoA pool to produce C24 and C26 fatty acids (Oh et al., 1997). To investigate the specificity of FARs, we expressed them in the *elo3Δ* mutant that is deficient in one of these elongases. There was a considerable increase in the synthesised fatty alcohols in *elo3Δ* mutant yeast transformed with the *HaFAR3* or *HaFAR4* genes, with *HaFAR3* producing a considerable increase in C20 and C22 fatty alcohols, and *HaFAR4* producing more C22 and C24 alcohols. In this host, *HaFAR2* did not produce any phenotype and *HaFAR5* did not increase total fatty alcohol content in the yeast. Hence, the FAR isoforms cloned from sunflower displayed high substrate specificity for saturated chain acyl-CoAs, with *HaFAR3* acting on C20 and C22 substrates, *HaFAR4* on C22, C24 and C26 and *HaFAR5* on C24 and C26, covering the range of fatty alcohols that are synthesised and present in sunflower seeds WEs. A loss in *HaFAR5* activity when expressed in the *elo3Δ* strain was not ruled out. To understand the lack of *HaFAR2* activity in yeast the sequence and three-dimensional structure of the proteins were studied.

All the cloned *HaFAR* genes retained the domains necessary for catalysis and the proteins were monomers, with a Rossmann-fold domain containing a NAD(P)H binding motif (GXXGXX(G/A)) and a YXXXX active site motif, followed by a FAR\_C domain that is present in all acyl-CoA reductases, even those acting on short or medium chain length substrates. Unlike the Rossmann-fold domain, the function of FAR\_C remained unclear even though both domains reside at the enzyme's surface close to one another. One of the most interesting aspects of these enzymes was their interaction with the acyl-CoA substrates. The docking of the 4 *HaFAR* forms with the 22:0-CoA substrate showed which regions of the enzyme were involved in the interaction with the

acyl substrates, highlighting a hydrophobic pocket at the surface of the enzyme close to the Rossmann-fold domain. This pocket is formed by hydrophobic and neutral amino acids like leucine, valine and tryptophan, and it does not differ considerably from that of *AtFAR3* (Fig. S5), suggesting that both act on similar acyl-CoA substrates. Based on these results, there is no evidence of *HaFAR2* dysfunctionality, which suggested that the cause of *HaFAR2* activity absence could be some kind of incompatibility with the yeast host.

One of the most controversial results obtained here is related to the subcellular location of the *HaFAR* enzymes. Sequence analysis of these proteins indicated that they do not have any transmembrane domain and the results from the software used to assess subcellular location was inconclusive in this respect, indicating a possible cytosolic localisation (Table S4). This contrasted with the subcellular localisation of other plant FAR homologues, such as those in Arabidopsis or wheat (Rowland et al., 2006; Wang et al., 2015) for which fluorescence labelling experiments revealed an ER localization. Here, the produced *HaFAR2*, *HaFAR3* and *HaFAR5* GFP constructs were agroinfiltrated into tobacco leaves along with the ER marker (CD3-959-mCherry: Nelson et al., 2007) and the cytosolic marker (NbRanBP1-RFP: Cho et al., 2008). *HaFAR1* and *HaFAR4* showed strong identity with *HaFAR2* and *HaFAR3*, suggesting a similar distribution. All *HaFARs* had a greater degree of overlap with the cytosolic marker, although this was not complete but it was greater than that observed with the ER marker. The cytosolic distribution of these enzymes differs from that of other enzymes involved in the synthesis of surface lipids, such as fatty acid elongases or wax synthases (WS), that are located in the ER (Cheng and Russell, 2004; Osei et al., 1989). The secondary structure and hydrophobic domains of *HaFARs* do not differ considerably from those of the Arabidopsis or wheat forms, such that any differences in their distribution cannot be ascribed to these features. It appears that FAR proteins are located in the interphase between the cytosol and ER, a distribution that is probably driven through protein-protein interactions. This would ensure that they are in the same locations as their substrates (cytosolic acyl-CoA pools) and in close contact with the other enzymes involved in WE synthesis that are located in the ER, like FAE and WS. In this regard, if *HaFARs* were peripheral membrane proteins depending on protein-protein interactions for their localisation, the absence of the interacting protein partners in the *Nicotiana benthamiana* system would hamper the production of clear localisation records.

Moreover, the possibility that the *HaFAR* localisation ambiguity is caused by certain artefacts induced by the fusion of fluorescent proteins should not be ruled out; therefore, this result needs to be confirmed via further experiments.

These data could be of interest to understand the WE synthesis in sunflower. In this regard, suppressing the synthesis of these lipids would ease sunflower oil refining, although it could make the seed more susceptible to pest attack, especially to fungal infection in humid climates (Lewandowska et al., 2020). In contrast, enhancing WE production could increase the resistance to fungal infection and produce more turbid oils, although this could be avoided by shelling the seeds prior to extraction. Alternatively, these WEs could serve to increase the production of sunflower waxes as a by-product.

## 5. Conclusions

Eight *HaFAR* genes homologous to *AtFAR3/CER4* were found in the sunflower database, which clustered into different groups related to the WE synthesis or the pollen cell wall. All genes except for *HaFAR7* were expressed in the seed hull during its development. The specificity of these enzymes in a WT strain of *Saccharomyces cerevisiae* showed that *HaFAR4* and *HaFAR5* produced saturated very long chain C24 and C26 fatty alcohols, whereas *HaFAR3* produced C20 and C22 alcohols when expressed in an elongase-deficient yeast mutant. In this mutant strain, *HaFAR4* also produced C22 alcohols in addition to its usual production of C24 alcohols. Based on their expression profile and specificity, these

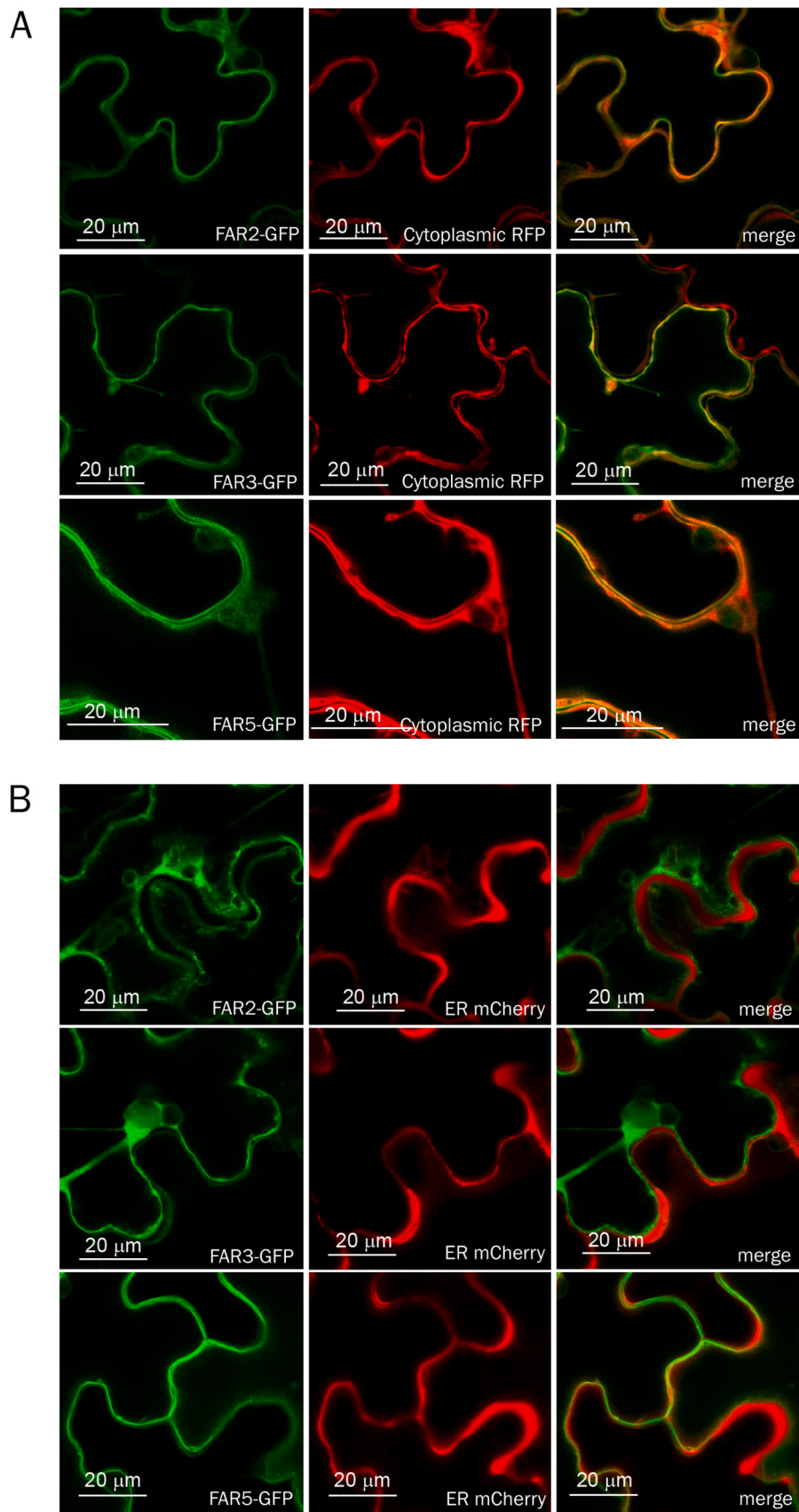


**Fig. 8.** Subcellular localisation of *HaFAR2*, *HaFAR3* and *HaFAR5*. (A) Confocal images of tobacco leaf epidermal cells expressing *HaFARs*-GFP and the cytosolic marker NbRanBP1-RFP. (B) Confocal images of tobacco leaf epidermal cells expressing *HaFARs*-GFP and the endoplasmic reticulum marker CD3-959 (ER-mCherry). Scale bar = 20  $\mu\text{m}$ .

three enzymes were likely to be involved in the synthesis of fatty alcohols in the sunflower hull, which range between C20 to C26. Although, they encode proteins containing an N-terminal Rossmann-fold and a C-terminal domain typical of fatty acid reductases, the area of interaction with the acyl substrate was established by docking with 22:0 acyl-CoA as a hydrophobic area located at the protein surface. The proteins produced from these genes were studied using fluorescent labelling and they were found to be preferentially localised in the cytosol.

### CRedit authorship contribution statement

**Martínez-Force Enrique:** Writing – review & editing, Visualization, Project administration, Methodology, Formal analysis, Conceptualization. **Halsey Kirstie:** Methodology, Investigation. **DeAndrés-Gil Cristina:** Writing – review & editing, Writing – original draft, Investigation, Conceptualization. **Villoslada-Valbuena Mónica:** Methodology, Investigation. **Moreno-Pérez Antonio J.:** Writing – review & editing, Supervision, Conceptualization. **Beaudoin Frédéric:** Writing – review & editing, Investigation, Conceptualization. **Kurup Smita:** Writing – review & editing, Investigation, Conceptualization. **Venegas-Calerón Mónica:** Writing – original draft, Supervision, Investigation, Funding acquisition, Conceptualization. **Salas Joaquín J.:** Writing – original draft, Supervision, Investigation, Funding acquisition, Conceptualization. **Garcés Rafael:** Visualization, Project administration, Methodology, Conceptualization.

### Declaration of Competing Interest

The authors declare that they have no known competing financial interests or personal relationships that could have appeared to influence the work reported in this paper.

### Data availability

No data was used for the research described in the article.

### Acknowledgments

We are grateful to the Advanced Optical Microscopy Facility of the Institute of Plant Biochemistry and Photosynthesis (IBVF) and Alicia Orea for her technical assistance. A.J. Moreno-Pérez is the recipient of a research contract from the VII PPIT-US. This work was funded by Spanish Ministerio de Ciencia e Innovación through the grants AGL2017 83449R and PID2020-113134RB-I00/MCIN/AEI/10.13039/501100011033, and the CSIC Project I-LINK 2021 Ref. LINKB20078.

### Appendix A. Supporting information

Supplementary data associated with this article can be found in the online version at [doi:10.1016/j.plantsci.2024.111992](https://doi.org/10.1016/j.plantsci.2024.111992).

### References

- M.G.M. Aarts, R. Hodge, K. Kalantidis, D. Florack, Z.A. Wilson, B.J. Mulligan, W. J. Stiekema, R. Scott, A. Pereira, The Arabidopsis MALE STERILITY 2 protein shares similarity with reductases in elongation/condensation complexes, *Plant J.: Cell Mol. Biol.* 12 (3) (1997) 615–623, <https://doi.org/10.1046/j.1365-313X.1997.00615.x>.
- H. Badouin, J. Gouzy, C.J. Grassa, F. Murat, S.E. Staton, L. Cottret, C. Lelandais-Brière, G. L. Owens, S. Carrère, B. Mayjonade, L. Legrand, N. Gill, N.C. Kane, J.E. Bowers, S. Hubner, A. Bellec, A. Bérard, H. Bergès, N. Blanchet, M.C. Boniface, D. Brunel, O. Catrice, N. Chaidir, C. Claudel, C. Donnadiet, T. Faraut, G. Fievet, N. Helmstetter, M. King, S.J. Knapp, Z. Lai, M.C. Le Paslier, Y. Lippi, L. Lorenzon, J.R. Mandel, G. Marage, G. Marchand, E. Marquand, E. Bret-Mestries, E. Morien, S. Nambesean, T. Nguyen, P. Pegot-Espagnet, N. Pouilly, F. Raftis, E. Sallet, T. Schiex, J. Thomas, C. Vandecasteele, D. Varès, F. Vear, S. Vautrin, M. Crespi, B. Mangin, J.M. Burke, J. Salse, S. Muñoz, P. Vincourt, L.H. Rieseberg, N.B. Langlade, The sunflower genome provides insights into oil metabolism, flowering and Asterid evolution, *Nature* 546 (7656) (2017) 148–152, <https://doi.org/10.1038/nature22380>.
- D.M. Becker, V. Lundblad, Manipulation of yeast genes, *Curr. Protoc. Mol. Biol.* 27 (1994) 13–17, <https://doi.org/10.1002/0471142727.mb1307s27>.
- E.G. Bligh, W.J. Dyer, A rapid method of total lipid extraction and purification, *Can. J. Biochem. Physiol.* 37 (8) (1959) 911–917, <https://doi.org/10.1139/o59-099>.
- T. Blum, S. Briesemeister, O. Kohlbacher, MultiLoc2: Integrating phylogeny and Gene Ontology terms improves subcellular protein localization prediction, *BMC Bioinforma.* 10 (2009) 274, <https://doi.org/10.1186/1471-2105-10-274>.
- R. Broughton, N. Ruiz-Lopez, K.L. Hassall, E. Martínez-Force, R. Garcés, J.J. Salas, F. Beaudoin, New insights in the composition of wax and sterol esters in common and mutant sunflower oils revealed by ESI-MS/MS, *Food Chem.* 269 (2018) 70–79, <https://doi.org/10.1016/j.foodchem.2018.06.135>.
- C. Camacho, G. Coulouris, V. Avagyan, N. Ma, J. Papadopoulos, K. Bealer, T.L. Madden, Blast+: Architecture and applications, *BMC Bioinforma.* 10 (2009) 421, <https://doi.org/10.1186/1471-2105-10-421>.
- M.G. Chacón, A.E. Fournier, F. Tran, F. Dittich-Domergue, I.P. Pulsifer, F. Domergue, O. Rowland, Identification of amino acids conferring chain length substrate specificities on fatty alcohol-forming reductases FAR5 and FAR8 from Arabidopsis thaliana, *J. Biol. Chem.* 288 (42) (2013) 30345–30355, <https://doi.org/10.1074/jbc.M113.499715>.
- M.C. Chalapud, E.R. Bäuml, A.A. Carelli, Characterization of waxes and residual oil recovered from sunflower oil winterization waste, *Eur. J. Lipid Sci. Technol.* 119 (2) (2017) 1500608, <https://doi.org/10.1002/ejlt.201500608>.
- S. Chang, J. Puryear, J. Cairney, A simple and efficient method for isolating RNA from pine trees, *Plant Mol. Biol. Report.* 11 (2) (1993) 113–116, <https://doi.org/10.1007/BF02670468>.
- W. Chen, X.H. Yu, K. Zhang, J. Shi, S. de Oliveira, L. Schreiber, J. Shanklin, D. Zhang, Male Sterile2 encodes a plastid-localized fatty acyl carrier protein reductase required for pollen exine development in Arabidopsis, *Plant Physiol.* 157 (2) (2011) 842–853, <https://doi.org/10.1104/pp.111.181693>.
- J.B. Cheng, D.W. Russell, Mammalian wax biosynthesis: I. Identification of two fatty acyl-coenzyme A reductases with different substrate specificities and tissue distributions, *J. Biol. Chem.* 279 (36) (2004) 37789–37797, <https://doi.org/10.1074/jbc.M406225200>.
- A.C. Chibnall, S.H. Piper, A. Pollard, E.F. Williams, P.N. Sahai, The constitution of the primary alcohols, fatty acids and paraffins present in plant and insect waxes, *Biochem. J.* 28 (6) (1934) 2189–2208, <https://doi.org/10.1042/bj0282189>.
- H.K. Cho, J.A. Park, H.S. Pai, Physiological function of NbRanBP1 in Nicotiana benthamiana, *Mol. Cells* 26 (3) (2008) 270–277.
- F. Dittich-Domergue, J. Joubès, P. Moreau, R. Lessire, S. Stymme, F. Domergue, The bifunctional protein TfFARAT from Tetrahymena thermophila catalyzes the formation of both precursors required to initiate ether lipid biosynthesis, *J. Biol. Chem.* 289 (32) (2014) 21984–21994, <https://doi.org/10.1074/jbc.M114.579318>.
- T.T.P. Doan, F. Domergue, A.E. Fournier, S.J. Vishwanath, O. Rowland, P. Moreau, C. C. Wood, A.S. Carlsson, M. Hamberg, P. Hofvander, Biochemical characterization of a chloroplast localized fatty acid reductase from Arabidopsis thaliana, *Biochim. Et. Biophys. Acta* 1821 (9) (2012) 1244–1255, <https://doi.org/10.1016/j.bbap.2011.10.019>.
- F. Domergue, M. Miklaszewska, The production of wax esters in transgenic plants: Towards a sustainable source of bio-lubricants, *J. Exp. Bot.* 73 (9) (2022) 2817–2834, <https://doi.org/10.1093/jxb/erac046>.
- F. Domergue, S.J. Vishwanath, J. Joubès, J. Ono, J.A. Lee, M. Bourdon, R. Alhattab, C. Lowe, S. Pascal, R. Lessire, O. Rowland, Three Arabidopsis fatty acyl-coenzyme A reductases, FAR1, FAR4, and FAR5, generate primary fatty alcohols associated with suberin deposition, *Plant Physiol.* 153 (4) (2010) 1539–1554, <https://doi.org/10.1104/pp.110.158238>.
- E. Fehling, K.D. Mukherjee, Acyl-CoA elongase from a higher plant (*Lunaria annua*): Metabolic intermediates of very-long-chain acyl-CoA products and substrate specificity, *Biochim. Et. Biophys. Acta* 1082 (3) (1991) 239–246, [https://doi.org/10.1016/0005-2760\(91\)90198-Q](https://doi.org/10.1016/0005-2760(91)90198-Q).
- K. Fujimoto, M. Hara, H. Yamada, M. Sakurai, A. Inaba, A. Tomomura, S. Katoh, Role of the conserved Ser-Tyr-Lys triad of the SDR family in sepiapterin reductase, *Chem. Biol. Interact.* 130–132 (1–3) (2001) 825–832, [https://doi.org/10.1016/S0009-2797\(00\)00238-6](https://doi.org/10.1016/S0009-2797(00)00238-6).
- R. Garcés, C. de Andrés-Gil, M. Venegas-Calerón, E. Martínez-Force, A.J. Moreno-Pérez, J.J. Salas, Characterization of sunflower seed and oil wax ester composition by GC/MS, a final evaluation, *LWT* 173 (2023) 114365, <https://doi.org/10.1016/j.lwt.2022.114365>.
- A. Grosdidier, V. Zoete, O. Michielin, Fast docking using the CHARMM force field with EADock DSS, *J. Comput. Chem.* 32 (10) (2011a) 2149–2159, <https://doi.org/10.1002/jcc.21797>.
- A. Grosdidier, V. Zoete, O. Michielin, SwissDock, a protein-small molecule docking web service based on EADock DSS, *Nucleic Acids Res.* 39 (Web Server issue) (2011b) W270–W277, <https://doi.org/10.1093/nar/gkr366>.
- T.A. Hall, BioEdit: A user-friendly biological sequence alignment editor and analysis program for Windows 95/98/NT, *Nucleic Acids Symp.* Ser. 41 (1999) 95–98, [https://doi.org/10.14601/Phytopathol\\_Mediterr-14998u1.29](https://doi.org/10.14601/Phytopathol_Mediterr-14998u1.29).
- J. Hallgren, K.D. Tsrigos, M. Damgaard Pedersen, J. Juan, A. Armenteros, P. Marcatili, H. Nielsen, A. Krogh, O. Winther, DeepTMHMM predicts alpha and beta transmembrane proteins using deep neural networks, *bioRxiv* (2022), 2022–2004.
- J. Jumper, R. Evans, A. Pritzel, T. Green, M. Figurnov, O. Ronneberger, K. Tunyasuvunakool, R. Bates, A. Žídek, A. Potapenko, A. Bridgland, C. Meyer, S.A. Kohli, A.J. Ballard, A. Cowie, B. Romera-Paredes, S. Nikolov, R. Jain, J. Adler, T. Back, S. Petersen, D. Reiman, E. Clancy, M. Zielinski, M. Steinegger, M. Pacholska, T. Berghammer, S. Bodensteiner, D. Silver, O. Vinyals, A.W. Senior, K. Kavukcuoglu, P. Kohli, D. Hassabis, Highly accurate protein structure prediction with AlphaFold, *Nature* 596 (7873) (2021) 583–589, <https://doi.org/10.1038/s41586-021-03819-2>.

- T.C.S. Kanya, L.J. Rao, M.C.S. Sastry, Characterization of wax esters, free fatty alcohols and free fatty acids of crude wax from sunflower seed oil refineries, *Food Chem.* 101 (4) (2007) 1552–1557, <https://doi.org/10.1016/j.foodchem.2006.04.008>.
- M. Karimi, A. Depicker, P. Hilson, Recombinational cloning with plant gateway vectors, *Plant Physiol.* 145 (4) (2007) 1144–1154, <https://doi.org/10.1104/pp.107.106989>.
- M. Karimi, D. Inzé, A. Depicker, GATEWAY™ vectors for Agrobacterium-mediated plant transformation, *Trends Plant Sci.* 7 (5) (2002) 193–195, [https://doi.org/10.1016/S1360-1385\(02\)02251-3](https://doi.org/10.1016/S1360-1385(02)02251-3).
- R. Kleiman, F.R. Earle, I.A. Wolff, Wax esters from sunflower oil tank settlings, *J. Am. Oil Chemists' Soc.* 46 (9) (1969) 505, <https://doi.org/10.1007/BF02544379>.
- A. Krishnan, B.A. McNeil, D.T. Stuart, Biosynthesis of fatty alcohols in engineered microbial cell factories: Advances and limitations, *Front. Biotechnol.* 8 (2020) 610936, <https://doi.org/10.3389/fbioe.2020.610936>.
- S. Kumar, G. Stecher, M. Li, C. Knyaz, K. Tamura, MEGA X: Molecular evolutionary genetics analysis across computing platforms, *Mol. Biol. Evol.* 35 (6) (2018) 1547–1549, <https://doi.org/10.1093/molbev/msy096>.
- K.D. Lardizabal, J.G. Metz, T. Sakamoto, W.C. Hutton, M.R. Pollard, M.W. Lassner, Purification of a jojoba embryo wax synthase, cloning of its cDNA, and production of high levels of wax in seeds of transgenic Arabidopsis, *Plant Physiol.* 122 (3) (2000) 645–655, <https://doi.org/10.1104/pp.122.3.645>.
- M. Lewandowska, A. Keyl, I. Feussner, Wax biosynthesis in response to danger: Its regulation upon abiotic and biotic stress, *N. Phytol.* 227 (3) (2020) 698–713, <https://doi.org/10.1111/nph.16571>.
- K.J. Livak, T.D. Schmittgen, Analysis of relative gene expression data using real-time quantitative PCR and the 2- $\Delta\Delta$ CT method, *Methods* 25 (4) (2001) 402–408, <https://doi.org/10.1006/meth.2001.1262>.
- F. Madeira, M. Pearce, A.R.N. Tivey, P. Basutkar, J. Lee, O. Edbali, N. Madhusoodanan, A. Kolesnikov, R. Lopez, Search and sequence analysis tools services from EMBL-EBI in 2022, *Nucleic Acids Res.* 50 (W1) (2022) W276–W279, <https://doi.org/10.1093/nar/gkac240>.
- J.G. Metz, M.R. Pollard, L. Anderson, T.R. Hayes, M.W. Lassner, Purification of a jojoba embryo fatty acyl-coenzyme A reductase and expression of its cDNA in high erucic acid rapeseed, *Plant Physiol.* 122 (3) (2000) 635–644, <https://doi.org/10.1104/pp.122.3.635>.
- M. Miklaszewska, A. Banaś, Biochemical characterization and substrate specificity of jojoba fatty acyl-CoA reductase and jojoba wax synthase, *Plant Sci.* 249 (2016) 84–92, <https://doi.org/10.1016/j.plantsci.2016.05.009>.
- A.J. Moreno-Pérez, J.M. Santos-Pereira, R. Martins-Noguerol, C. DeAndrés-Gil, M. A. Troncoso-Ponce, M. Venegas-Calerón, R. Sánchez, R. Garcés, J.J. Salas, J.J. Tena, E. Martínez-Force, Genome-wide mapping of histone H3 lysine 4 trimethylation (H3k4me3) and its involvement in fatty acid biosynthesis in sunflower developing seeds, *Plants* 10 (4) (2021) 706, <https://doi.org/10.3390/plants10040706>.
- B.K. Nelson, X. Cai, A. Nebenführ, A multicolored set of in vivo organelle markers for co-localization studies in Arabidopsis and other plants, *Plant J.: Cell Mol. Biol.* 51 (6) (2007) 1126–1136, <https://doi.org/10.1111/j.1365-3113X.2007.03212.x>.
- C.S. Oh, D.A. Toke, S. Mandala, C.E. Martin, ELO2 and ELO3, homologues of the *Saccharomyces cerevisiae* ELO1 gene, function in fatty acid elongation and are required for sphingolipid formation, *J. Biol. Chem.* 272 (28) (1997) 17376–17384, <https://doi.org/10.1074/jbc.272.28.17376>.
- P. Osei, S.K. Suneja, J.C. Laguna, M.N. Nagi, L. Cook, M.R. Prasad, D.L. Cinti, Topography of rat hepatic microsomal enzymatic components of the fatty acid chain elongation system, *J. Biol. Chem.* 264 (12) (1989) 6844–6849, [https://doi.org/10.1016/s0021-9258\(18\)83507-4](https://doi.org/10.1016/s0021-9258(18)83507-4).
- S. Paul, K. Gable, F. Beaudoin, E. Cahoon, J. Jaworski, J.A. Napier, T.M. Dunn, Members of the Arabidopsis FAE1-like 3-ketoacyl-CoA synthase gene family substitute for the elop proteins of *Saccharomyces cerevisiae*, *J. Biol. Chem.* 281 (14) (2006) 9018–9029, <https://doi.org/10.1074/jbc.M507723200>.
- T. Paysan-Lafosse, M. Blum, S. Chuguransky, T. Grego, B.L. Pinto, G.A. Salazar, M. L. Bileschi, P. Bork, A. Bridge, L. Colwell, J. Gough, D.H. Haft, I. Letunić, A. Marchler-Bauer, H. Mi, D.A. Natale, C.A. Orengo, A.P. Pandurangan, C. Rivoire, C. J.A. Sigrist, I. Sillitoe, N. Thanki, P.D. Thomas, S.C.E. Tosatto, C.H. Wu, A. Bateman, InterPro in 2022 (<https://doi.org/https://doi.org/>), *Nucleic Acids Res.* 51 (D1) (2023) D418–D427, <https://doi.org/10.1093/nar/gkac993>.
- E.F. Pettersen, T.D. Goddard, C.C. Huang, G.S. Couch, D.M. Greenblatt, E.C. Meng, T. E. Ferrin, UCSF Chimera - A visualization system for exploratory research and analysis, *J. Comput. Chem.* 25 (13) (2004) 1605–1612, <https://doi.org/10.1002/jcc.20084>.
- G. Rivarola, M.C. Añón, A. Calvelo, Crystallization of waxes during sunflower seed oil refining, *J. Am. Oil Chemists' Soc.* 62 (10) (1985) 1508–1513, <https://doi.org/10.1007/BF02541904>.
- O. Rowland, F. Domergue, Plant fatty acyl reductases: Enzymes generating fatty alcohols for protective layers with potential for industrial applications, *Plant Science, Elsevier Ireland Ltd.*, 2012, <https://doi.org/10.1016/j.plantsci.2012.05.002>.
- O. Rowland, H. Zheng, S.R. Hepworth, P. Lam, R. Jetter, L. Kunst, CER4 encodes an alcohol-forming fatty acyl-coenzyme A reductase involved in cuticular wax production in Arabidopsis, *Plant Physiol.* 142 (3) (2006) 866–877, <https://doi.org/10.1104/pp.106.086785>.
- N. Saitou, M. Nei, The neighbor-joining method: A new method for reconstructing phylogenetic trees, *Mol. Biol. Evol.* 4 (4) (1987) 406–425.
- J.J. Salas, M.A. Botoello, R. Garcés, Food uses of sunflower oil, in: E. Martínez-Force, N. T. Dunford, J.J. Salas (Eds.), *Sunflower: Chemistry, production, processing, and utilization*, AOCs Press, 2015, pp. 441–464, <https://doi.org/10.1016/B978-1-893997-94-3.50020-9>.
- J. Shi, H. Tan, X.H. Yu, Y. Liu, W. Liang, K. Ranathunge, R.B. Franke, L. Schreiber, Y. Wang, G. Kai, J. Shanklin, H. Ma, D. Zhang, Defective pollen wall is required for anther and microspore development in rice and encodes a fatty acyl carrier protein reductase, *Plant Cell* 23 (6) (2011) 2225–2246, <https://doi.org/10.1105/tpc.111.087528>.
- V. Thumulari, J. Almagro Armenteros, A.R. Johansen, H. Nielsen, O. Winther, DeepLoc. 2.0: Multi-label subcellular localization prediction using protein language models Vineet, *Nucleic Acids Res.* 50 (April) (2022) 1–7, <https://doi.org/10.1093/nar/gkac278>.
- G.E. Tusnady, I. Simon, The HMMTOP transmembrane topology prediction server, *Bioinformatics* 17 (9) (2001) 849–850, <https://doi.org/10.1093/bioinformatics/17.9.849>.
- M. Wang, Y. Wang, H. Wu, J. Xu, T. Li, D. Hegebarth, R. Jetter, L. Chen, Z. Wang, Three TaFAR genes function in the biosynthesis of primary alcohols and the response to abiotic stresses in *Triticum aestivum*, *Sci. Rep.* 6 (1) (2016) 25008, <https://doi.org/10.1038/srep25008>.
- Y. Wang, M. Wang, Y. Sun, Y. Wang, T. Li, G. Chai, W. Jiang, L. Shan, C. Li, E. Xiao, Z. Wang, FAR5, a fatty acyl-coenzyme A reductase, is involved in primary alcohol biosynthesis of the leaf blade cuticular wax in wheat (*Triticum aestivum* L.), *J. Exp. Bot.* 66 (5) (2015) 1165–1178, <https://doi.org/10.1093/jxb/eru457>.
- R.M. Willis, B.D. Wahlen, L.C. Seefeldt, B.M. Barney, Characterization of a fatty acyl-CoA reductase from *Marinobacter aquaeolei* VT8: A bacterial enzyme catalyzing the reduction of fatty acyl-CoA to fatty alcohol, *Biochemistry* 50 (48) (2011) 10550–10558, <https://doi.org/10.1021/bi2008646>.